

Single Image Enhancement Using Inter-channel Correlation

Jin Kim¹, Soowoong Jeong¹, Yong-Ho Kim¹, and Sangkeun Lee²

¹ The graduate school of Advanced Imaging Science, Multimedia and Film, Chung-Ang University / Korea (R.O.K)
{zin, imgrecog, petrus0321}@mmc.cau.ac.kr

² The graduate school of Advanced Imaging Science, Multimedia and Film, Chung-Ang University / Korea (R.O.K)
sangkny@cau.ac.kr

* Corresponding Author: Sangkeun Lee

Received July 14, 2012; Revised July 29, 2012; Accepted August 20, 2012; Published June 30, 2013

* Regular Paper

Abstract: This paper proposes a new approach for enhancing digital images based on red channel information, which has the most analogous characteristics to invisible infrared rays. Specifically, a red channel in RGB space is used to analyze the image contents and improve the visual quality of the input images but it can cause unexpected problems, such as the over-enhancement of reddish input images. To resolve this problem, inter-channel correlations between the color channels were derived, and the weighting parameters for visually pleasant image fusion were estimated. Applying the parameters resulted in significant brightness as well as improvement in the dark and bright regions. Furthermore, simple contrast and color corrections were used to maintain the original contrast level and color tone. The main advantages of the proposed algorithm are 1) it can improve a given image considerably with a simple inter-channel correlation, 2) it can obtain a similar effect of using an extra infrared image, and 3) it is faster than other algorithms compared without artifacts including halo effects. The experimental results showed that the proposed approach could produce better natural images than the existing enhancement algorithms. Therefore, the proposed scheme can be a useful tool for improving the image quality in consumer imaging devices, such as compact cameras.

Keywords: Image enhancement, Fusion, Contrast correction, Inter-channel correlation

1. Introduction

Nowadays, to capture a scene, a general digital camera produces millions or tens of millions of pixels using CCD or CMOS, which converts light into an electronic signal, and an A/D converter that changes an analog signal to a digital signal. The dynamic range of general compact digital cameras is narrower than that of human visual observations because of the mechanic limitations of CCD and CMOS. Many image enhancement algorithms have been evaluated to solve this problem [1-9]. The research can be categorized into two classes: homogeneous and heterogeneous approaches. The homogeneous scheme uses a single or multiple images from the same wavelength range in the light spectrum, whereas the heterogeneous one uses multiple images from different wavelength ranges.

The Retinex method [4], which is a representative

homogeneous scheme, is based on the experimental fact that the images received are given by illumination and reflectance components. Therefore, the method enhances an image by reducing the illumination component and only presenting the reflectance. In particular, the illumination is estimated using the Gaussian kernel for each scale, and is eliminated from the original image. Furthermore, its logarithmic computation effectively compresses the dynamic range. On the other hand, this approach requires complicated computation and a long processing time, which makes it difficult for hardware implementation. In addition, employing a Gaussian kernel for estimating an illumination factor might cause halo effects. Fusion with several differently exposed images [19] also falls within this category. The kernel requires additional procedures for solving registration and vibration problems. For an alternative approach (i.e. heterogeneous scheme), one

study evaluated a fusion-based enhancement algorithm combining IR (Infrared light Range) and VR (Visible light Range) images [10-13]. The CCD or CMOS in the general compact digital cameras can receive a wider range of information over visible light because it is designed to sense the near-infrared and visible ranges.

Near-infrared rays have wavelengths between 700 and 1200 nm, which is longer than that of visible light (350-750 nm). Therefore, infrared rays have an advantage in transmission because it is less scattered in the air particles, and IR images provide useful information that is not observed in VR images. Therefore, using the information of infrared rays for image enhancement can help improve the image properly [10]. On the other hand, fusing VR and IR images can cause several problems. First, fusion-based approaches of combining two IR and VR images require pixel-to-pixel registration; imperfect registration results in undesired blurring. Second, an extended exposure time due to light blocking by IR filters in the camera can generate noise in the image. Third, it is difficult to set the focus for an IR image. Therefore, this paper introduces a new single image enhancement approach using the red channel of an input image, which has the closest spectrum region to the near-infrared wavelength among the other VR image channels: R, G, and B. The basic idea is that the property of the red channel is somehow similar to that of near-infrared rays because they are overlapped in certain areas of the electromagnetic spectrum. The proposed approach has a problem of not being able to reflect the information existing only in an IR image, but it is more effective in enhancing the details and brightness in the dark areas than the existing fusion-based algorithms using the IR image. In addition, the inter-channel correlation between the color channels is presented to resolve the over-enhancement problem, which can occur when applying the proposed approach to high reddish images. A main procedure in this study is that the estimated illumination component of a red channel is combined with the luminance channel of an input image using a weighting function. This fused result might be low in contrast and suffer from color distortion because the main procedure is done in a luminance channel. Therefore, appropriate adjustments including contrast and

color corrections are needed to make the image more natural to the human eyes.

This paper is structured as follows. Section 2 describes the proposed scheme followed by an experimental comparison with other existing algorithms in Section 3. The conclusion with some discussions is given in Section 4.

2. Proposed Method

Fig. 2 presents the overall scheme of the proposed algorithm. First, the inter-channel correlation between color channels is explained to reduce the over-enhancement of red-tone images. Next, red channel processing is presented to improve the visual quality of the input images. Simple contrast and color corrections are then formulated to preserve the original contrast level and color tone, respectively.

2.1 Inter-Channel Correlation

A red channel was used in an input image because it contains useful information that exists in an IR image compared to other channels, because it is closer to IR in the light spectrum. A red component fused with a luminance channel described in the following section gives better improvement than any other channel combinations. The proposed method actively uses a luminance channel in CIE Lab [20] color space to reflect the property of a red channel. On the other hand, using a red channel to improve the visual quality may result in over-enhancement of the images including an excessive red component. This problem can be resolved using the inter-channel correlation C between color channels, and is defined as

$$C_1 = \overline{\mu_r} / \overline{\mu_g}, C_2 = \overline{\mu_r} / \overline{\mu_b}, C_3 = \overline{\mu_r} / \overline{\mu_l}$$

and

$$C = \min\{C_1, C_2, C_3\} \tag{1}$$

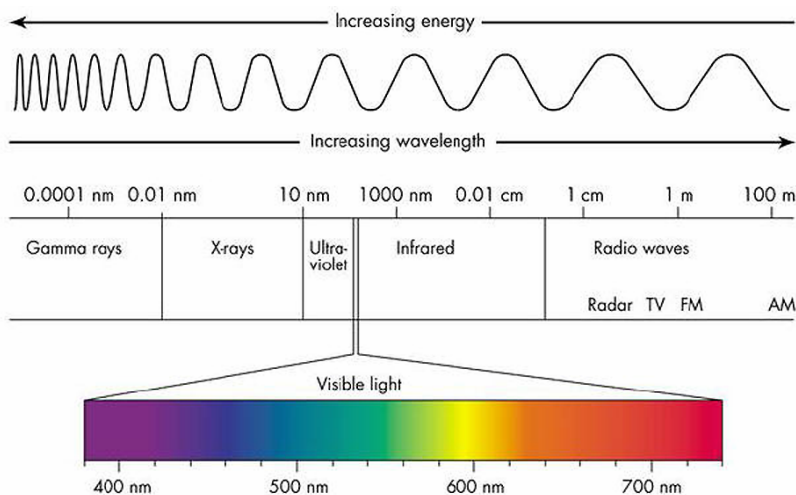


Fig. 1. Wavelength of light spectrum.

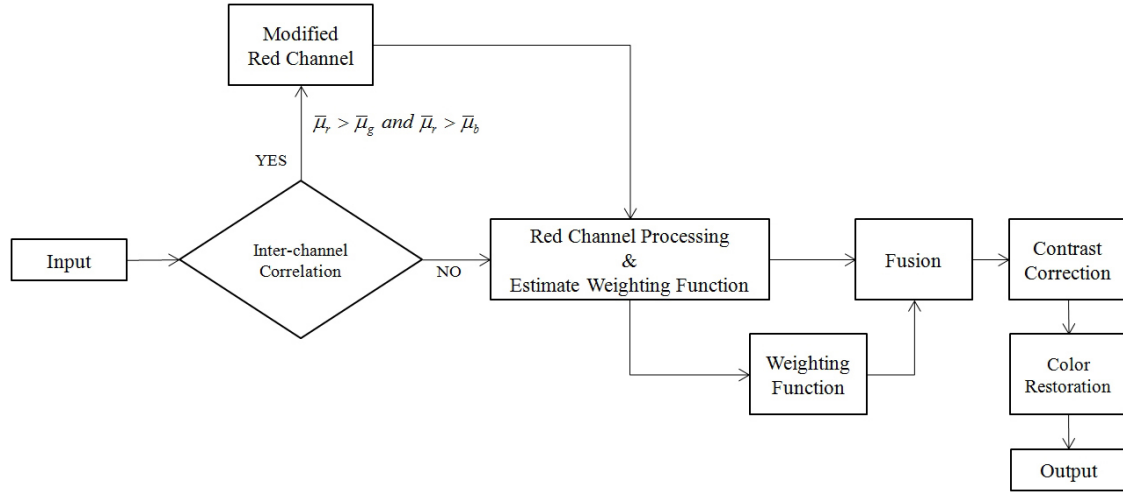


Fig. 2. Block diagram of the proposed scheme.

where $\bar{\mu}_x$ denotes the average value of each channel, $x(= R, G, B, L)$, whereas C_η ($\eta = 1, 2, 3$) indicates the degree of significance in the intensity average of the red channel to the other channels. That is, C denotes the smallest difference among red and other channels. A modified red component \tilde{O}_{red} was calculated as follows:

$$\tilde{O}_{red} = \begin{cases} C \cdot O_l, & \text{if } \bar{\mu}_r > \bar{\mu}_g \text{ and } \bar{\mu}_r > \bar{\mu}_b \\ O_{red}, & \text{otherwise} \end{cases} \quad (2)$$

where if the given conditions are met, the luminance O_l replaces the original red component with a weighting factor C . Otherwise, the original red channel O_{red} is used as it is.

2.2 Red Channel Processing

The modified red channel \tilde{O}_{red} can be expressed as a multiplication of the illumination I_r and reflectance R_r components [4] as follows:

$$\tilde{O}_{red} = I_r \cdot R_r \quad (3)$$

Bilateral Filter (BF) is used in this study to estimate the illumination factor of a given red channel, and the estimated illumination component is defined as

$$\tilde{I}_r = \frac{1}{W_p} \sum_{\mathbf{q} \in S} G_{\sigma_s}(\|\mathbf{p} - \mathbf{q}\|) G_{\sigma_r}(|\tilde{O}_{red\mathbf{p}} - \tilde{O}_{red\mathbf{q}}|) \tilde{O}_{red\mathbf{q}} \quad (4)$$

where W_p is the normalization factor, and G_{σ_s} , and G_{σ_r} are the spatial and radiometric weighting functions for distance and intensity, respectively. That is, it conducts the convolution operation while maintaining the edges changing rapidly according to the brightness of the image. The

bilateral filter considers the rapid changes in brightness, and it adaptively adjusts the filtering so that any Halo artifacts can be minimized at the later fusion process. After estimating the illumination component, it is inverted to use as an indicator of the degree of enhancement of the given image at the fusion step as follows:

$$inv\tilde{I}_r = 1 - \tilde{I}_r \quad (5)$$

This equation can be used to effectively compress the dynamic range of an input image and improve the details in both dark and bright regions if necessary. After red channel processing, a weighting coefficient ω for fusion is obtained from the modified red and luminance channels in the input image as follows:

$$\omega = \begin{cases} \max\{\omega_1, \omega_2\}, & \text{if } \bar{\mu}_l < \tau \\ \min\{\omega_1, \omega_2\}, & \text{otherwise} \end{cases} \quad (6)$$

and

$$\begin{aligned} \omega_1 &= \max(inv\tilde{I}_r) - \bar{\mu}_{inv\tilde{I}_r} \\ \omega_2 &= \max(O_l) - \bar{\mu}_l \end{aligned} \quad (7)$$

where $\bar{\mu}_{inv\tilde{I}_r}$ and $\bar{\mu}_l$ are the average values of the inverted illumination of red channel and luminance component, respectively. The value of ω changes adaptively according to the mean input luminance. The threshold τ is the critical value that determines the degree of brightness and darkness of the input image. To determine the value, 300 natural images were taken under 3 different exposures: dark; normal; and highlight (-2 EV, 0 EV, and +2 EV), as shown in Fig. 3. Fig. 4 shows the mean intensity of the L channel in the *CIE Lab*. A critical point exists for the given images to be dark or bright to the human eye. In other words, an image with a value below τ ($=0.4$) belongs to a very dark image, whereas an image above τ belongs to either optimal exposed or highlighted image. Therefore, a

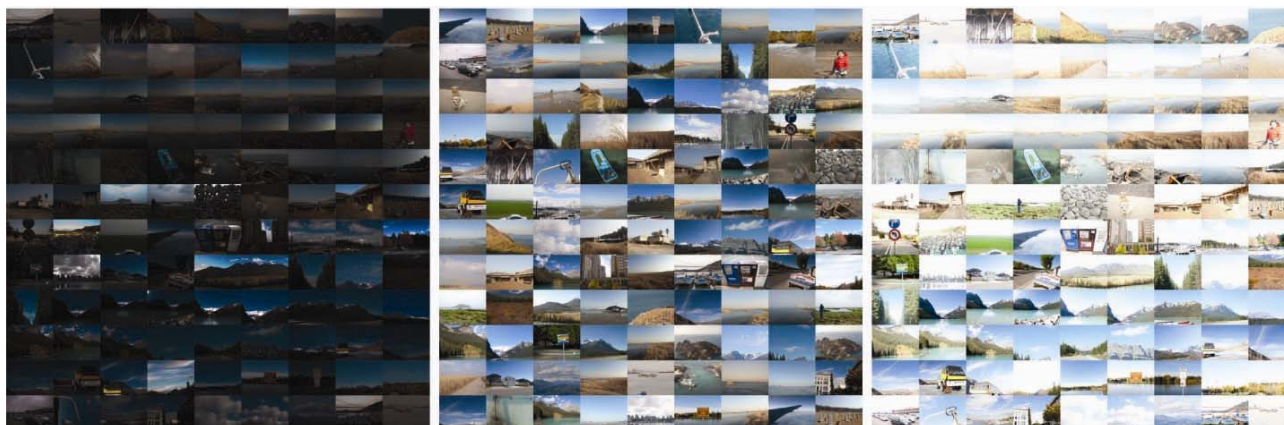


Fig. 3. Different exposure images. From the left to right: -2 EV, 0 EV, and +2 EV.

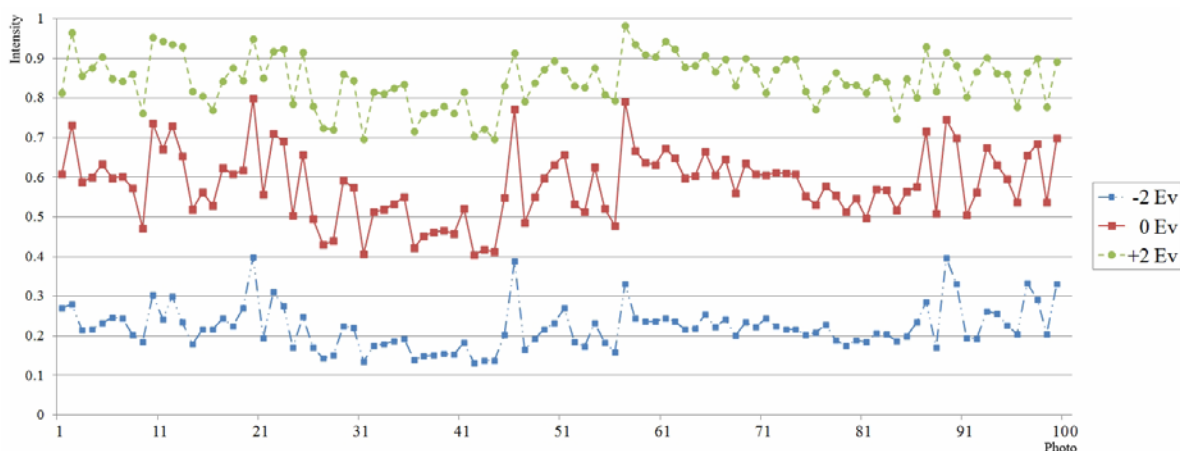


Fig. 4. Mean intensity values of the L channel to determine a critical point τ .



Fig. 5. (a) Original, (b) Image fusion result, (c) contrast correction, (d) color restoration ($\alpha = 0.1, \gamma = 0.2$).

weighting coefficient ω selects the larger value of ω_1 and ω_2 if the mean luminance of the input image is lower than τ , and otherwise the smaller one is chosen for proper enhancement. The modified L channel O_L is formulated by combining an original L channel O_l and an inverted red channel illumination component, $inv\tilde{I}_r$, according to the fusion coefficient ω as follows:

$$O_L = \begin{cases} (1-\omega) \cdot inv\tilde{I}_r + \omega \cdot O_l, & \text{if } \bar{\mu}_l < \tau \\ \omega \cdot inv\tilde{I}_r + (1-\omega) \cdot O_l, & \text{otherwise} \end{cases} \quad (8)$$

In this event, the output provides better details in the dark and bright areas, but may suffer from the generation of a low contrast and unnatural appearance, as shown in Fig. 5(b). Therefore, a simple contrast correction was employed to enhance the resulting appearance.

2.3 Contrast Correction and Color Restoration

This section describes simple contrast and color correction schemes. They were performed to adjust the contrast level and correct the distortions in color for the resulting image. The former was conducted only in the L

channel while the latter was done in RGB color space.

A simple contrast correction was calculated from stretching the 10% upper and lower brightness level of the given image histogram as follows:

$$\hat{O}_L = \frac{O_L - \text{Min}}{\text{Max} - \text{Min}} \times 100 \quad (9)$$

with

$$\begin{aligned} \text{Min} &= \min(O_L) - (\min(O_L) \times 0.1) \\ \text{Max} &= \max(O_L) + (\max(O_L) \times 0.1) \end{aligned} \quad (10)$$

Fig. 5(c) shows the result of the proposed scheme after simple contrast adjustment. On the other hand, this approach may have color distortion because one color channel, e.g. luminance channel, has been adjusted to improve the image details. To resolve this problem and restore the original color distribution, a simple color restoration factor, CR_i ($i = R, G, B$), was first defined as

$$CR_i(x, y) = O_i(x, y) / \sum_{i \in \{R, G, B\}} O_i(x, y) \quad (11)$$

where $O_i(x, y)$ denotes each channel $i (= R, G, B)$ of the input image. The final output for each channel was calculated after considering the color restoration factor as follows:

$$O_{CR}^i(x, y) = \hat{O}_i(x, y) + (CR_i(x, y) \cdot \alpha) - \gamma \quad (12)$$

where, α and γ indicate the saturation level and the brightness adjustment of the image, respectively. In practice, they are assigned to the range of [0 1]. Both the saturation and brightness increased with increasing α . On

the other hand, the increased brightness at this point does not affect the visual appearance of the image positively. Therefore, the value γ plays an important role in maintaining the saturation and brightness level as much as possible. Fig. 5 shows the resulting image of each step for the proposed algorithm. In particular, Figs. 5(c) and (d) illustrated the results after applying a simple contrast stretch and a color restoration to the fused result (b), respectively.

3. Experimental Results

To evaluate the performance of the proposed approach, all comparing algorithms were implemented with a numerical computing programming language (Matxxx 2008b), and the experiment was conducted using Windows 7 on 2.66 GHz i5 CPU and 3 GB RAM. The experiments were performed in twofold: comparison with a single image-based enhancement, such as the Retinex algorithm; and a comparison with the VR and IR fusion-based methods. Quality metrics, (Enhancement Measure Entropy) [15], Discrete entropy [16], and Brenner's measure [17], which are objective and subjective methods were employed to evaluate the single image-based enhancement. In addition, the processing time was also compared. On the other hand, for the comparison with the hybrid fusion approaches, only an observation-based visual evaluation was provided in this study because there was no standard evaluator [14]. For the first test, six distinctive images, which were taken from clear sky, outdoors, portrait, and a back lighted photography with excessive red tone, were selected, as shown in Fig. 6. The MSRRCR approach [4] is based on the experiment, in which an image was composed of illumination and reflectance components. This approach improves the image by



Fig. 6. Test images captured under a range of conditions.



Fig. 7. Comparable resultant images for six test images. From the top (1st row) to bottom (4th row): Original; MSRCR; NRCIR; and The proposed approach.

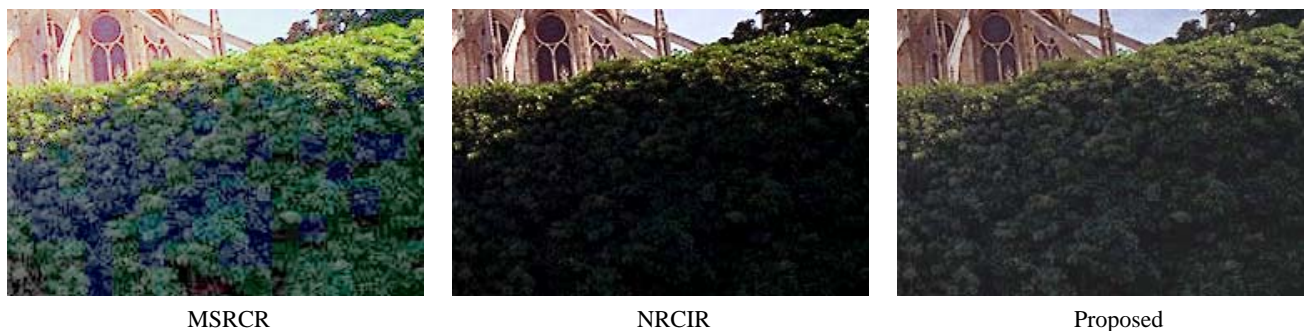


Fig. 8. Partially enlarged images in Fig. 7 (e) for MSRCR, NRCIR, and the proposed algorithm.

adjusting the reflectance component by estimating the illumination one from applying multi-scale Gaussian kernels. Unlike the Retinex algorithm employing a Gaussian kernel for each scale, the NRCIR uses a global tone mapping process and modifies the filter shape [1] to prevent Halo artifacts occurring in MSRCR. Contrast rescaling and map-based image enhancement is then accompanied to make the final image more natural and pleasant. The difference between the existing algorithms and the proposed algorithm is that the Red channel was analyzed and modified to enhance the given high contrast images. Fig. 7 presents the comparable results of MSRCR, NRCIR, and the proposed scheme. MSRCR increases both the overall brightness and details, but its over-enhancement results in unnatural color appearance. In addition, the result of the NRCIR image produces a natural output without over correction or color distortion. On the other hand, it is difficult to see the improvements in the details, particularly in dark areas. In contrast, the proposed method provides better details both in the dark and light regions while maintaining its natural appearance. For a

better illustration of the comparable results, the insets of the lower wood area in Fig. 7(e) are shown in Fig. 8.

Again, MSRCR causes excessive noise and color distortion due to over-enhancement, whereas NRCIR results in more natural but less overall improvement. The proposed approach, however, shows clear details while maintaining the natural appearance of the given image.

Table 1 also compares the processing time. The proposed scheme is approximately 10 to 30 times on average faster than NRCIR and MSRCR, respectively. This is because MSRCR undergoes complicated computations for each channel, and NRCIR takes many steps to improve luminance channel alone.

EME (enhancement measure of entropy), discrete entropy, and Brenner’s measures were employed for an objective evaluation of the compared algorithms. EME measures the degree of local contrast losses, such as image degradation by noise and a decrease in the edges. The high EME score indicates high quality image. The quality was computed by the largest value of function χ for $k_1 \times k_2$ blocks as follows:

TABLE 1. Processing Time comparisons (Sec).

Input	MSRCR	NRCIR	Proposed
(a)	23.46	9.55	1.07
(b)	18.31	9.31	1.05
(c)	22.2	9.37	1.06
(d)	39.04	16.10	1.62
(e)	46.59	18.02	1.69
(f)	32.85	12.83	1.28

$$EME = \max \chi \left(\frac{1}{k_1 k_2} \sum_{i=1}^{k_1} \sum_{j=1}^{k_2} \frac{I_{\max;i,j}^{\omega}}{I_{\min;i,j}^{\omega}} \log \frac{I_{\max;i,j}^{\omega}}{I_{\min;i,j}^{\omega}} \right) \quad (13)$$

where $I_{\max;k,l}^{\omega}$ and $I_{\min;k,l}^{\omega}$ indicate the minimum and maximum brightness within the block size of the image $\omega_{i,j}$. Discrete entropy is defined as

$$E = - \sum_{i=0}^{255} (p(s_i) \times \log_2 p(s_i)) \quad (14)$$

Here, S_i denotes brightness value of the sequence i from the resulting image, i.e. the degree of entropy for the output image histogram is measured. Similarly, Brenner's measure indicates the degree of sharpness and is defined as

$$F_{br} = \sum_x \sum_y (I(x, y) - I(x + 2, y))^2 \quad (15)$$

Tables 2 to 4 show the EME, discrete entropy, and Brenner's measure, respectively, for each algorithm.

TABLE 2. EME (Enhancement Measure Entropy).

	Original	MSRCR	NRCIR	Proposed
(a)	32.37	9.57	30.28	22.53
(b)	12.58	4.01	11.67	9.08
(c)	15.46	4.10	14.49	12.40
(d)	32.00	9.52	19.84	21.02
(e)	29.80	9.20	24.94	16.59
(f)	27.61	10.75	4.62	9.66

TABLE 3. Discrete Entropy.

	Original	MSRCR	NRCIR	Proposed
(a)	7.11	7.71	7.56	7.38
(b)	6.96	7.21	7.47	7.21
(c)	7.17	7.77	7.60	7.24
(d)	7.23	7.68	7.65	7.40
(e)	7.34	7.60	7.53	7.57
(f)	7.62	7.48	7.83	7.78

TABLE 4. Brenner's measure (10^6).

	Original	MSRCR	NRCIR	Proposed
(a)	121.54	105.38	147.42	125.93
(b)	47.39	44.19	67.39	54.42
(c)	78.60	66.33	99.93	72.66
(d)	198.18	177.62	224.27	185.94
(e)	252.72	277.45	298.20	237.92
(f)	206.34	162.57	238.18	194.91

Unfortunately, it was very difficult to determine the consistency for the image quality. As observed from the previous results including Fig. 8, the existing algorithms



VR Image



IR Image



CP



LP



NSCT



Proposed

Fig. 9. Competitive images from fusion-based approaches and the proposed algorithm.

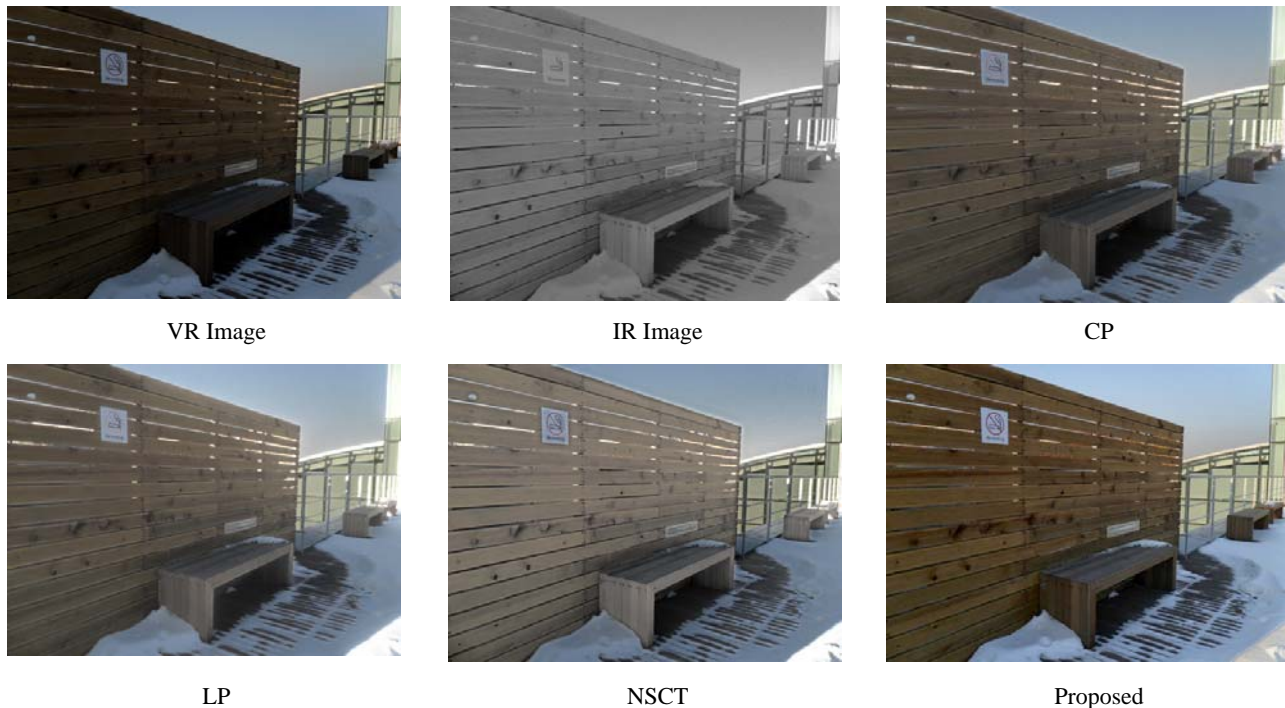


Fig. 10. More outputs from the existing algorithms using both IR and VR images while the proposed one using only a VR image.

showed over or under enhancement compared to the proposed scheme. Therefore, the results from the qualitative metrics cannot be used as absolute quality metrics.

In the second test, comparative experiments were carried out using IR and VR image fusion approaches for image enhancement. Two representative approaches were selected from the VR and IR fusion-based approaches, pyramidal decomposition (DP) [11] and non-subsampled contourlet transform (NSCT) [13]. Pyramidal decomposition divides an image into high and low frequency components using a Gaussian pyramid, and compares the characteristic value of the image to fuse with the larger or average value. The NSCT scheme extends the previous NSCT [12] to correct Gibb's phenomenon that occurs in the general discontinuity signals for the wavelet-based method, and enhances the input with fusing with high, low frequency and directional information without going through the down sampling process.

This paper compared the proposed algorithm with two pyramid decomposition-based approaches, which are contrast pyramid decomposition (CP) and Laplacian pyramid decomposition (LP), and one NSCT-based scheme, as shown in Figs. 9 and 10. The fusion-based methods using an extra IR image showed improvement in the details in the sky region compared to the original VR image. In contrast, as expected, the proposed scheme did not improve the details because it only used a single VR image that did not contain detailed information of the sky. On the other hand, the proposed method showed outstanding performance in enhancing the details in the dark region compared to the fusion-based approaches, even without an extra IR image. Fig. 10 provides an additional example to show some problems of the fusion-

based schemes. The fusion-based methods caused color distortion and halo artifacts around the large edges, whereas the details were improved in the dark areas. Even imperfect pixel registration can result in undesired image blurring. On the other hand, the proposed scheme showed a more natural appearance of an image in color without any halo or image blurring. Therefore, the proposed method can be used as a simple and effective tool for a single image-based enhancement in related fields, such as compact cameras/videos and surveillance applications.

4. Conclusion

This paper proposes a scheme for image enhancement using the special and useful properties of the red channel, which is similar to that of infrared rays. A comparison with the existing MSRCR scheme revealed the proposed algorithm to show less distortion in colors and a minimized Halo effect around large edges. In addition, the imaging details were improved both in the dark and highlighted region while maintaining the natural appearance of an image.

In particular, compared to IR and VR image fusion approaches, the details of the dark area were improved considerably, even though the improvement in the details visible only in the infrared image is limited. Nevertheless, it is believed that the proposed scheme can be a useful alternative to fusion-based approaches that require VR and IR images for image enhancement. Furthermore, the simplicity and effectiveness of the proposed algorithm can be applied directly to consumer products, such as compact cameras without complicated hardware modification.

Acknowledgements

This work was supported by Basic Science Research Program through the National Research Foundation of Korea(NRF) funded by the Ministry of Education, Science and Technology(2013-029824, 2011-0015901) and BK21 plus project.

References

- [1] L. Meylan and S. Susstrunk, "Bio-inspired Color Image Enhancement," *IS&T/SPIE Electronic Imaging 2004: Human vision and electronic imaging IV*, vol. 5292, pp. 46-56, San Jose CA, USA, 2004. [Article\(CrossRefLink\)](#)
- [2] S. Lee, V. H. S. Ha, and Y. H. Kim, "Dynamic Range Compression and Contrast Enhancement for Digital Images in the Compressed Domain," *Journal of Optical Engineering*, vol. 45, no. 2, pp. 1 – 14, Feb. 2006. [Article\(CrossRefLink\)](#)
- [3] S. Chen and A. Beghdadi, "Natural Rendering of Color Image based on Retinex," *IEEE 16th International Conference on Image Processing*, pp.1813-1816, Nov. 2009. [Article\(CrossRefLink\)](#)
- [4] Z. Rahman, D. J. Jobson, and G. A. Woodell, "Retinex Processing for Automatic Image Enhancement," *Journal of Electronic Imaging*, vol. 13, no. 1, Jan. 2004. [Article\(CrossRefLink\)](#)
- [5] Z. Rahman, D.J.Jobson, and G. A. Woodell, "Multiscale Retinex for Color Image Enhancement," *International Conference on Image Processing*, 1996. [Article\(CrossRefLink\)](#)
- [6] L. Meylan and S. Susstrunk, "High Dynamic Range Image Rendering with a Retinex-based Adaptive Filter," *IEEE Trans. Image Processing*, vol. 15, no. 9, pp. 2820-2830, 2006. [Article\(CrossRefLink\)](#)
- [7] E. H. Land and J. McCann, "Lightness and Retinex Theory," *Journal of the Optical Society of America*, vol. 61, no. 1, pp. 1-11, 1971. [Article\(CrossRefLink\)](#)
- [8] B. Funt, F. Ciurea, and J. MacCann, "Retinex in Matlab," *Proc. IS&T/SID 8th Color Imag. Conf.*, pp. 112, 2000. [Article\(CrossRefLink\)](#)
- [9] W. C. Kao, L. Y. Chen, and S. H. Wang, "Tone Reproduction in Color Imaging Systems by Histogram of Macro Edges," *IEEE Trans. Consumer Electronics*, vol. 52, no. 2, pp. 682-688, May 2006. [Article\(CrossRefLink\)](#)
- [10] J. S. Kim, Y. H. Kim, and S. K. Lee, "Image Enhancement through Weighting Function Estimation with Infrared Image," *International SoC Design Conference*, Nov. 2010. [Article\(CrossRefLink\)](#)
- [11] Toet A, Ruyven L. V, and Velaton J, "Merging Thermal and Visual Images by a Contrast Pyramid," *Optical Engineering*, vol. 28, no. 7, pp. 789-792, 1989. [Article\(CrossRefLink\)](#)
- [12] L. Cunha, J. Zhou, and M. N. Do, "The Nonsampled Contourlet Transform: Theory, Design, and Applications," *IEEE Trans. Image Processing*, vol. 15, no. 10, pp. 3089-3101, May 2005. [Article\(CrossRefLink\)](#)
- [13] Z. Xin and L. Rui-an, "Infrared and Visible Image Fusion Enhancement Technology based on Multi-scale Directional Analysis," *the 2nd International Congress on Image and Signal Processing*, pp. 1-3, Oct. 2009. [Article\(CrossRefLink\)](#)
- [14] S. S. Agaian, K. Panetta, and A. M. Grigoryan, "Transform-based Image Enhancement Algorithms with Performance Measure," *IEEE Trans. Image Processing*, vol. 10, no. 3, pp. 367-382, Mar. 2001. [Article\(CrossRefLink\)](#)
- [15] S. S. Agaian, K. Panetta, and A. M. Grigoryan, "A New Measure of Image Enhancement," *Presented at the IASTED Int. Conf. Signal Processing Communication*, pp. 19-22, Marbella, Spain, Sep. 2000. [Article\(CrossRefLink\)](#)
- [16] C. Wang and Z. Ye, "Brightness Preserving Histogram Equalization with Maximum Entropy: A Variational Perspective," *IEEE Trans. Consumer Electronics*, vol. 51, no. 4, pp. 1326-1334, Nov. 2005. [Article\(CrossRefLink\)](#)
- [17] M. S. Shyu and J. J. Leou, "A Genetic Algorithm Approach to Color Image Enhancement," *Pattern Recognition*, vol. 31, no. 7, pp. 871-880, 1998. [Article\(CrossRefLink\)](#)
- [18] H. Li, B. S. Manjunath, and S. K. Mitra, "Multisensor Image Fusion using the Wavelet Transform," *Graphical Models and Image Processing*, vol. 57, no. 3, pp. 234-245, 1995. [Article\(CrossRefLink\)](#)
- [19] W. C. Kao, C. C. Hsu, L. Y. Chen, C. C. Kao, and S. H. Chen, "Integrating Image Fusion and Motion Stabilization for Capturing Still Images in High Dynamic Range Scenes," *IEEE Trans. Consumer Electronics*, vol. 52, no. 3, pp. 735-740, Aug. 2006. [Article\(CrossRefLink\)](#)
- [20] M. D. Fairchild, *Color Appearance Models*. John Wiley and Sons. 2005. [Article\(CrossRefLink\)](#)



Jin Kim received the B.S. degree in Photography and Film from Gyeongju University, Gyeongju, Korea in 2008, and his M.S. degree in Imaging Engineering from Chung-Ang University, Seoul, Korea, in 2012. His research interests include Image Enhancement, Tone Mapping and Image Fusion.



Soowoong Jeong received his B.S. degree in Multimedia from Namseoul University, Cheonan, Korea in 2010m and his M.S. degree in Image Engineering from Chung-Ang University, Seoul, Korea, in 2012. He is currently pursuing a Ph.D. degree at Chung-Ang University. His research interests include image enhancement, dehazing, and retinex.



Yong-Ho Kim received a B.S. degree in Computer and Information from Hanseo University, Seosan, Korea in 2008, and his M.S. degree in Imaging Engineering from Chung-Ang University, Seoul, Korea, in 2010. He is currently pursuing a Ph.D. degree at Chung-Ang University. His research interests include Object recognition via graph matching, Image retrieval and stereo coding.



Sangkeun Lee received the B.S. and M.S. degrees in Electronic Engineering from Chung-Ang University, Seoul, Korea, in 1996 and 1999, respectively, and the Ph.D. degree in Electrical and Computer Engineering from Georgia Institute of Technology, Atlanta, GA, in 2003. He is an associate professor of the graduate school of Advanced Imaging Science, Multimedia & Film at Chung-Ang University, Seoul, Korea. From 2003 to 2008, he was a staff research engineer with the Digital Media Solutions Lab, Samsung Information Systems America, Irvine, CA, where he was involved in the development of video processing and enhancement algorithms (DNIE) for Samsung's HDTV. His current research and development interests include digital video/image processing, especially video analysis/synthesis, denoising, compression for HDTV and multimedia applications, and content-based video representation and abstraction. He is a senior member of the IEEE.